Electronic Supplementary Information

Nano-Tungsten Carbide Decorated Graphene as Co-catalyst for Enhanced Hydrogen Evolution on Molybdenum Disulfide

Ya Yan,[a] *Baoyu Xia,*[a] *Xiaoying Qi,*[c] *Haibo Wang,*[a] *Rong Xu,*[a] *Jing-Yuan Wang,*[b] *Hua Zhang,*[c] *and Xin Wang**[a]

[a] School of Chemical and Biomedical Engineering, Nanyang Technological University,50 Nanyang Avenue, 639798 ,Singapore. Fax: +65 67947553; E-mail: WangXin@ntu.edu.sg

[b] Residues and Resource Reclamation Centre, Nanyang Technological University

[c] School of Materials Science and Engineering, Nanyang Technological University

Experimental details

Synthesis of nano-WC: For a typical synthesis of nano-WC, a certain amount (50-80 mg) of as-prepared WO_3 nanorods as mentioned in our previous paper[1] was transferred into a tube furnace for reduction-carburization. The whole system was first purged with argon gas to completely remove any air before heating. The argon gas

was then switched off and a mixture of CH_4 (20 mL min^{-1}) and H_2 (80 mL min^{-1}) was fed to the furnace. In the meantime, the furnace was first heated to 600 °C with a ramp rate of 5 °C min^{-1} and then to 800 °C at a rate of 2 °C min^{-1} and kept at this temperature for 3h. After that, the furnace was cooled down to a temperature of 700 °C. The supply of the carburizing agent was switched off and argon was used to purge the furnace again. The furnace was further cooled down to room temperature.

Synthesis of Graphene oxide (GO): Graphene oxide (GO) was synthesized from natural graphite powder by a modified Hummers' method.

Synthesis of the nano-WC/GO hybrids: Hybrid of WC/GO was obtained by adding as-prepared nano-WC to GO dispersed in 15 mL of Dimethylformamide (DMF) /H_2O (10:1) mixture. The mixture was sonicated in ice water bath for accumulated 30 min in a program of 1s on 1s off and then stirred at room temperature overnight. In order to investigate the effect of WC content in the WC/GO hybrid co-catalyst on the electrocatalytic hydrogen evolution activity of MoS_2,the weight percentages of WC to GO were varied from 0 to 100 (0, 20, 25, 33.3 and 100 wt%) by varying the weight of nano-WC, the resulting samples were labeled as xW(100-x)G, where W and G refer to WC and graphene, respectively, and x = 0, 20, 25, 33.3 and 100, respectively.

Synthesis of layered-MoS_2/WC/RGO composite: The composite samples were synthesized by a solvothermal method. $(NH_4)_2MoS_4$ was used as the MoS_2 source and was added to the 15 mL thoroughly mixed WC/GO hybrid GO. The mixture was sonicated at room temperature for approximately 20 min until a clear and

homogeneous solution was achieved. Then, 0.2 ml of $N_2H_4 \bullet H_2O$ was added and this obtained solution mixture was further sonicated for 10 min before transferred to a 50 mL Teflon-lined autoclave with a Teflon liner and kept at 210 °C for 18 h. The resulting precipitate was collected, washed thoroughly with distilled water followed by a rinse in ethanol, and then dried at 60 °C for 12 h. Similarly, a series of the MoS_2/WC/RGO composites were prepared by using the *x*W(100-*x*)G as co-catalyst under the same conditions but replacing 25W75G with *x*W(100-*x*)G. Blank MoS_2 was also prepared following the same procedure as above except for the first addition of WC/GO hybrid co-catalyst. The detailed data are listed in Table S1. Moreover, in order to further investigate the content effect of the WC/RGO (25W75G) co-catalyst on the electrocatalytic hydrogen evolution activity of MoS_2, the weight ratio of 25W75G/MoS_2 was changed from 15wt % to 50wt % by varying the amount of 25W75G (see Table S2). For the purpose of comparison, 30%-25W75G/MoS_2 mixture was prepared by simple mechanical mixing of the pristine MoS_2 and 30 wt% of 25W75G without the solvothermal process.

Characterization: All transmission electron microscopy (TEM), high-resolution (HR)TEM images and element mapping were taken from JEOL JEM 2100F, while the field emission scanning electron microscopy (FESEM) images and energy-dispersive X-ray spectroscopy (EDX) spectra were taken on a JEOL JSM 6700F. XRD analysis of different samples was carried out on a X-ray diffractometer (Bruker AXS D8, Cu Kλ, λ = 1.5406 Å, 40 kV and 20 mA). Raman spectra were collected via a Renishaw Ramanscope in the backscattering configuration using 514

nm (2.41 eV) laser wavelengths over five random spots on the powers. X-ray photoelectron spectroscopy (XPS) spectrum was measured on a VG Escalab 250 spectrometer equipped with an Al anode (Al Kα = 1846.6 eV). The specific surface area and pore size distribution of the samples were evaluated in Autolab-6B (Quantachrome Instruments) using the liquid nitrogen adsorption/desorption method. All the samples were degassed at 120 °C for 2 hours before the measurements. The BET surface area was determined using adsorption data in the relative pressure (P/P_0) range of 0.05-0.25. The desorption branch was used to determine the pore size distribution *via* the Barret-Joyner-Halender (BJH) method. The nitrogen adsorption volume at the relative pressure (P/P_0) of 0.95 was used to determine the single-point pore volume and the average pore size. Thermo gravimetric analysis (TGA) and the derived differential thermogravimetric (DTA) experiments were conducted on a PerkinElmer Diamond TG/DTA equipment. The sample was first kept at 100 °C for 30 min to remove moisture and then was heated up to 1000 °C under high purity air flow (50 sccm) in a ramp of 10 °C/min while its weight was monitored. Atomic force microscope (AFM) with a MPF3D microscope from Asylum Research was used in this paper.

Electrochemical measurements: All electrochemical measurements were conducted on an Autolab PGSTAT302 potentiostat (Eco Chemie, Netherlands) in a three-electrode cell at room temperature. A Pt foil (4.0 cm^2) and a saturated calomel electrode (SCE) were used as counter and reference electrodes, respectively. The working electrode was prepared on a glass carbon (GC) disk as the substrate.

Typically, a mixture containing 2.0 mg catalyst, 2.5 mL ethanol and 0.5 mL Nafion solution (0.05 wt%, Gashub) was ultrasonicated for 15 min to obtain a well-dispersed ink. Then 20 μl of the catalyst ink (containing 13 μg of catalyst) was loaded onto a glassy carbon electrode of 4 mm in diameter (loading ~ 0.104 mg/cm^2). The presented current density refers to the geometric surface area of the glass carbon electrode. Linear sweep voltammetry with scan rate of 5 mV s^{-1}was conducted in 0.5 M H_2SO_4. The working electrodes were mounted at a rotating disc electrode with a rotating rate of 1000 rpm during the test. In all experiments, the electrolyte solutions were purged with N_2 for 15 min prior to the experiments in order to remove oxygen. During the measurements, the headspace of the electrochemical cell was continuously purged with N_2. AC impedance measurements were carried out in the same configuration at η= 0.15 V from 10^5-0.02 Hz with an AC voltage of 5 mV. Commercial Pt/C (20 wt %) from E-TEK was measured as received. All the potentials reported in our manuscript were referenced to a reversible hydrogen electrode (RHE) by adding a value of (0.241+0.059 pH) V.

Table S1. Effects of WC/RGO co-catalyst content in the MoS_2/WC/RGO electrocatalysts on the HER activity according to polarization measurements.

Sample[a]	Composition	Tafel slope [mV / decade][b]	Onset potential [V] [c]
100M/0(W-G)	100MoS_2+0(WC/RGO)	106	-0.14
85M/15(W-G)	85MoS_2+15(WC/RGO)	74	-0.13
80M/20(W-G)	80MoS_2+20(WC/RGO)	78	-0.13
70M/30(W-G)	70MoS_2+30(WC/RGO)	41	-0.11
60M/40(W-G)	60MoS_2+40(WC/RGO)	60	-0.15
50M/50(W-G)	50MoS_2+50(WC/RGO)	51	-0.16

[a] W-G samples contains 25%WC and 75% of RGO in the co-catalyst.

[b] Calculated from the linear portion of the plot in the potential range of 150 mV-200 mV.

[c] The onset potential at which the hydrogen evolution occurred measured versus RHE.

Table S2. Effects of WC/RGO weight ratio on the HER activity according to polarization measurements.

Sample[a]	Composition	Tafel slop [mV / decade][b]	Onset potential [V] [c]
M/0W-100G	MoS_2+RGO	47	-0.13
M/33.3W-66.7G	MoS_2+33.3WC-66.7RGO	47	-0.12
M/25W-75G	MoS_2+25WC-75RGO	41	-0.11
M/20W-80G	MoS_2+20WC-80RGO	45	-0.13
M/100W-0G	MoS_2+WC	54	-0.12

[a] All composite samples contain 70% of MoS_2 and 30% of co-catalyst in the composite electrocatalyst.

[b] Calculated from the linear portion of the plot in the potential range of 150 mV-200 mV.

[c] The onset potential at which the hydrogen evolution occurred measured versus RHE.

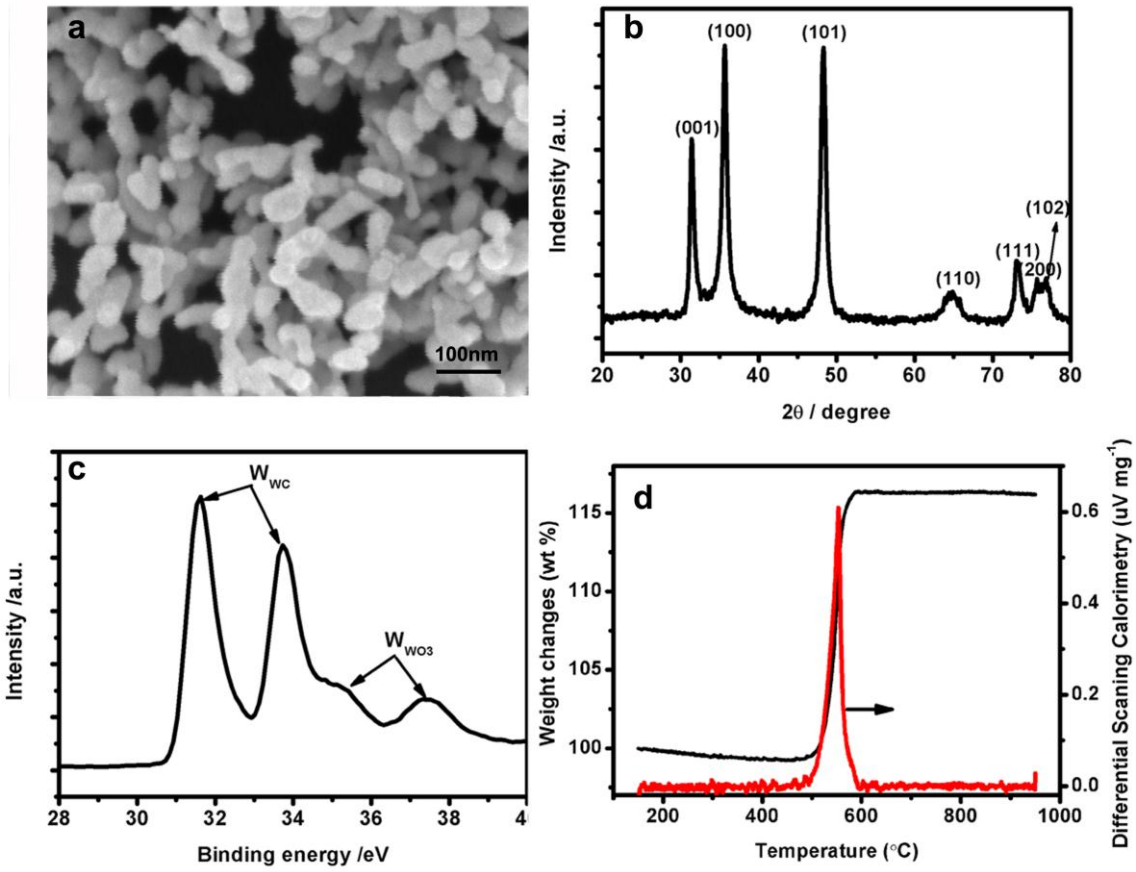

Figure S1. FESEM images (a), XRD pattern (b), XPS W4f spectra (c) and TGA-DSC (d) of the nano-WC obtained in the CH_4/H_2 mixtures at 800 °C for 3h.

The as-prepared WC nanoparticles exhibits an interesting string-like morphology with average size of 35 nm. XRD pattern demonstrated the material was a hexagonal WC (PDF # 25-1047. From XPS spectrum, the $W4f_{7/2}$ and the $W4f_{5/2}$ peaks corresponding to the binding energy of 31.6 and 33.7eV are assigned to the tungsten carbide.[2] It also demonstrates the oxygen-modified W on the particle's surface at 35.7 and 37.2 eV which could come from the thin WO*x* film that was formed in air at nanometer level, which is hardly detectable by XRD.[3] TG analysis of the nano-WC under air shows that there is a very slight weight loss (~0.5%) during the heating range of 150-500°C, which could be from undesirable amorphurous carbon. Beyond

this temperature range, an obvious weight increase caused by the oxidation of WC is observed from 500-600°C, which is consistent with the reported fact that oxidation of WC starts at 500–600 °C.[4] The above results could indicate the relativly high purity of the nano-WC precusor.

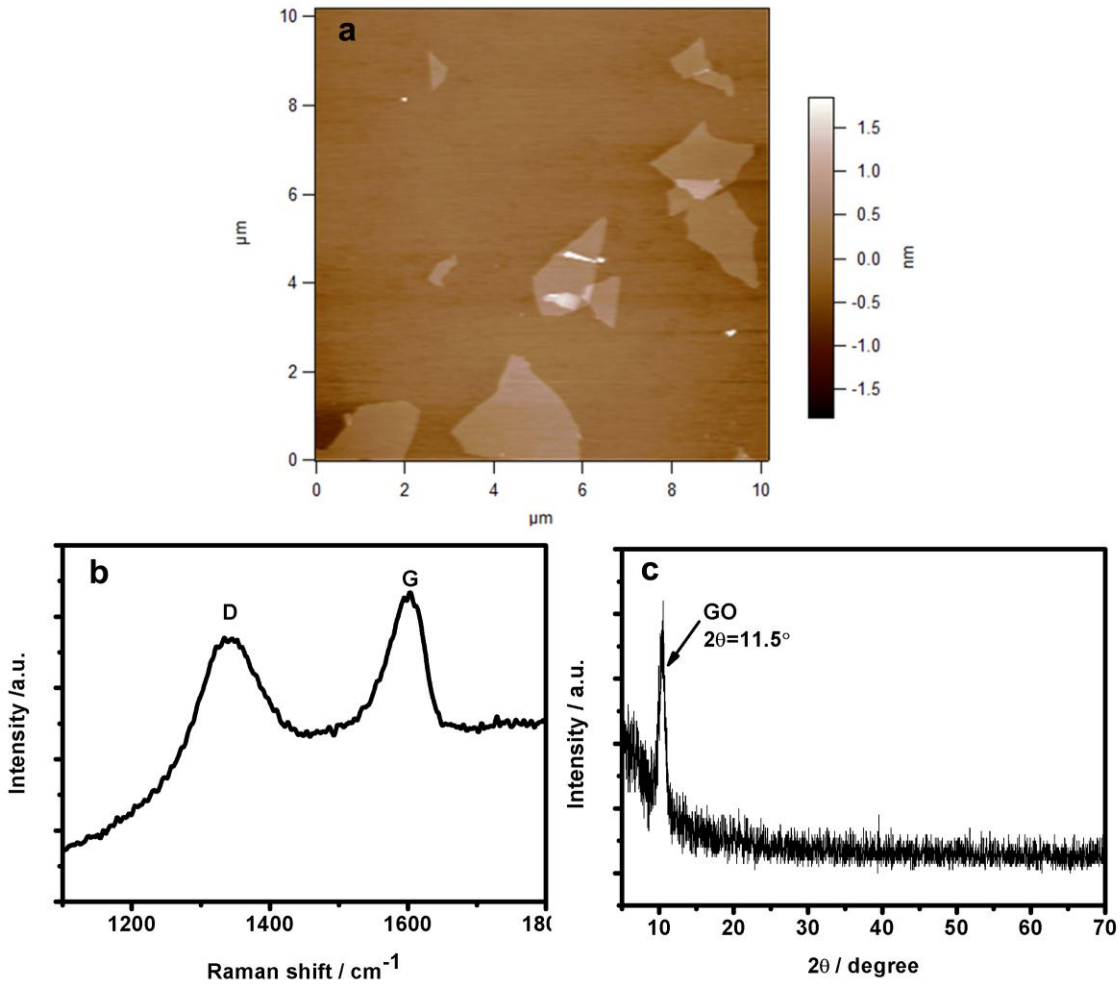

Figure S2. AFM image (a), Raman spectrum (b) and XRD pattern (c) of the prepared graphene oxide sheets as starting material.

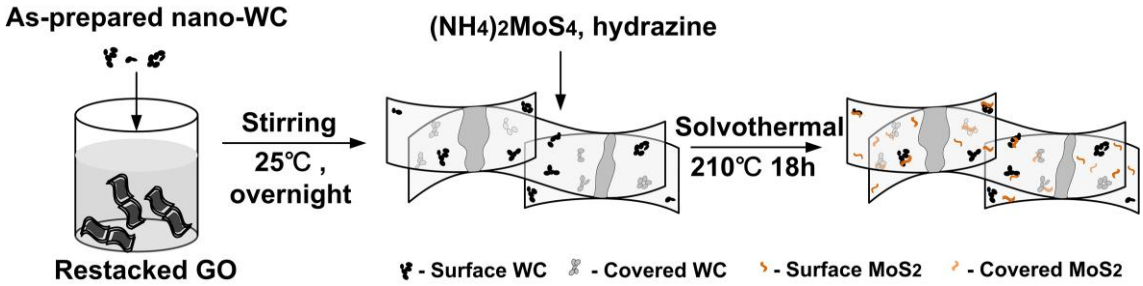

Figure S3. Schematic illustration of the synthesis of MoS_2/WC/RGO composite.

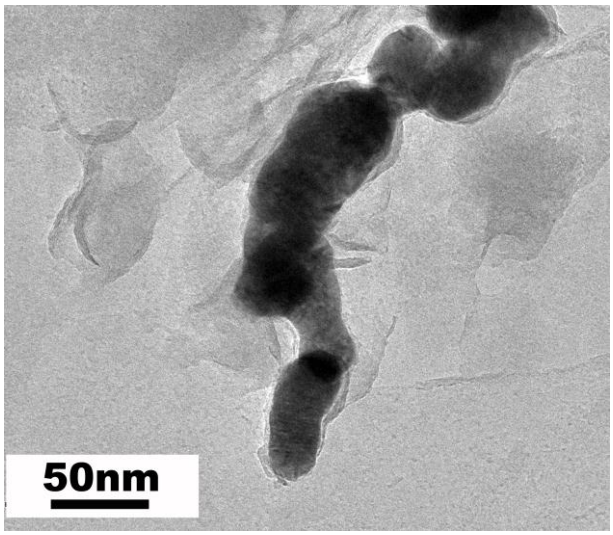

Figure S4. TEM image of the selected area of the MoS_2/WC/RGO composite for element mapping.

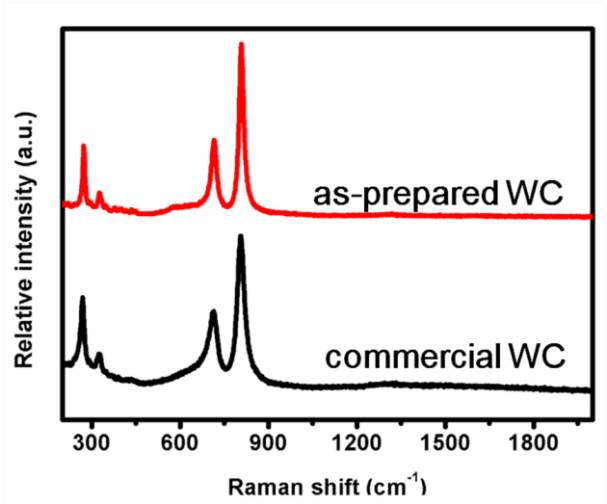

Figure S5. Raman spectra of self-prepared WC and commercial WC. The characteristic peaks of the as-prepared WC are consistent with the commercial one.

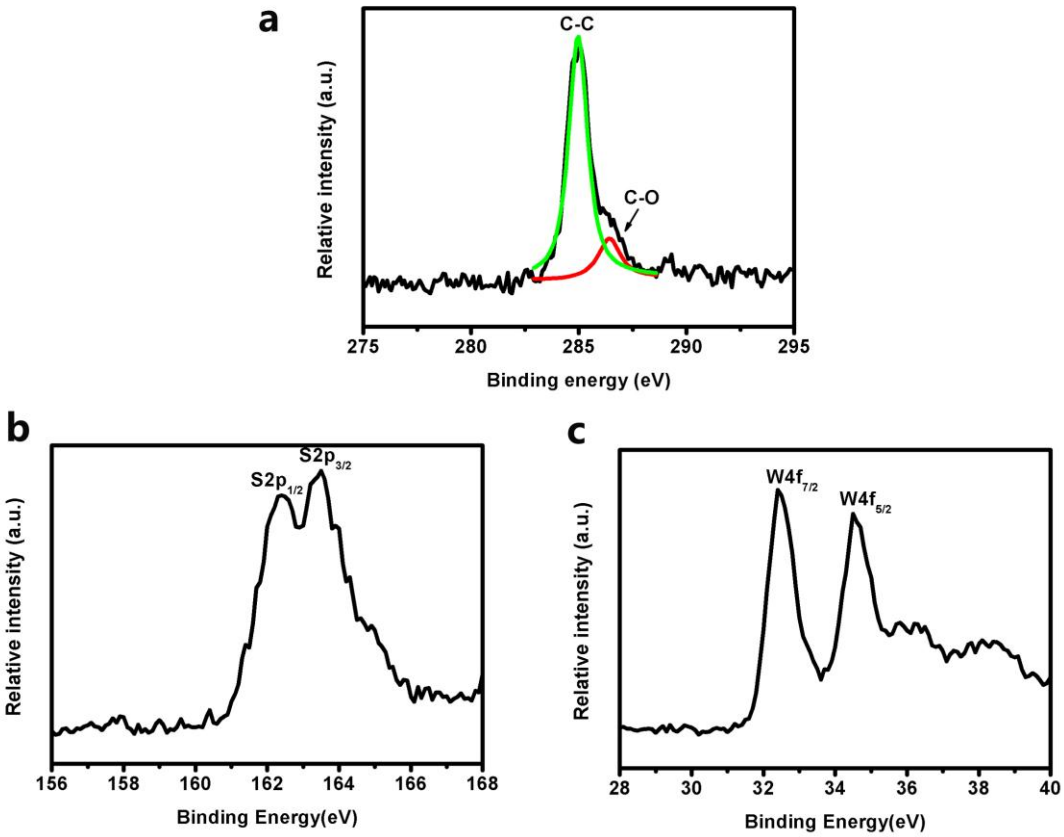

Figure S6. High-resolution XPS spectra of MoS_2/WC/RGO composites. (a) C 1s,(b) S2p and (c) W 4f spectrum.

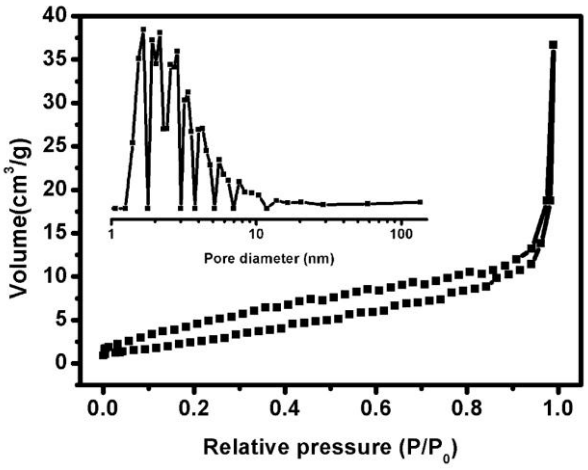

Figure S7. N_2 adsorption/desorption isotherms and the corresponding BJH pore-size distribution (inset) of nano-WC. The pore diameter distribution was determined from the desorption branch.

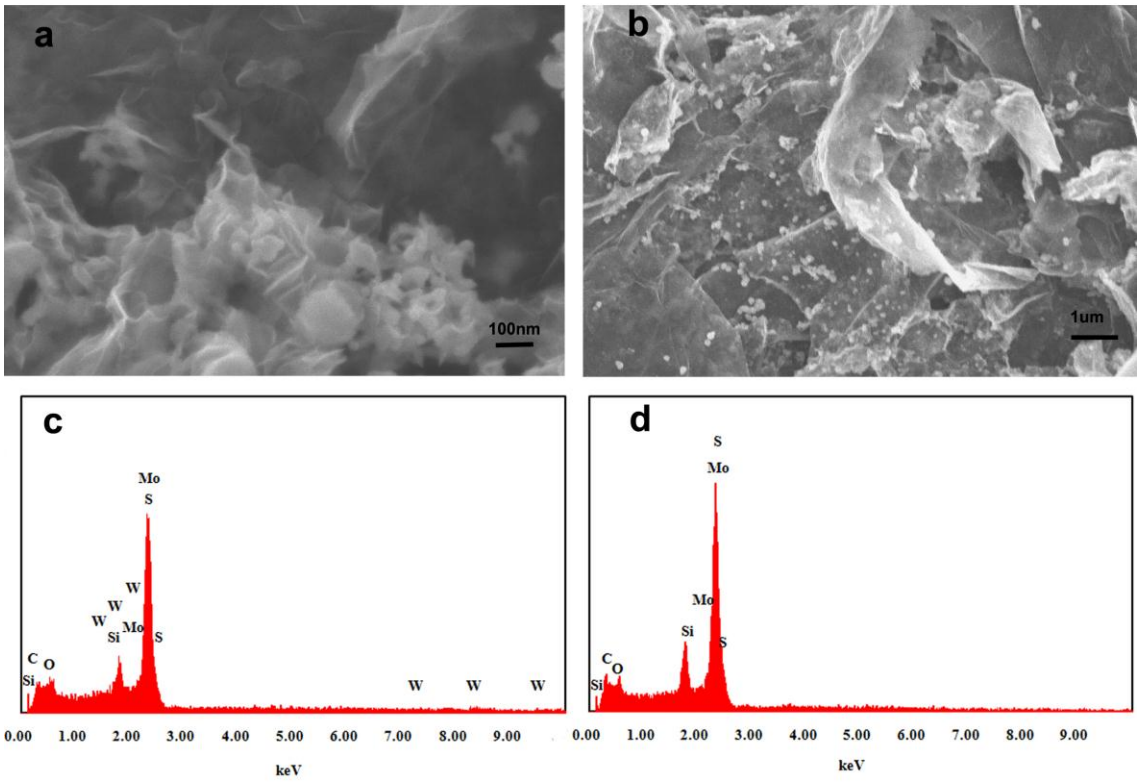

Figure S8. FESEM images and EDS spectra of MoS_2/WC/RGO composites (70M/30(W-G)) (a, c) and MoS_2/RGO hybrid (70M/30G) (b, d), respectively.

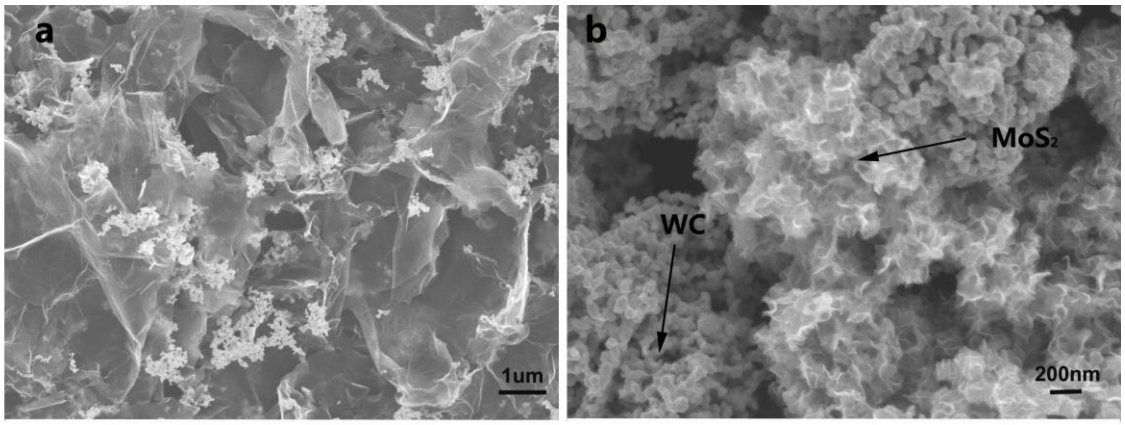

Figure S9. FESEM images of (a) nano-WC/RGO, (b) MoS_2/nano-WC hybrid.

Control experiment was also conducted in the absence of RGO by following the exactly same procedure, which resulted in the aggregation of MoS_2 particles and WC particles in separate regions (Figure S9b) and low activities and low activities.

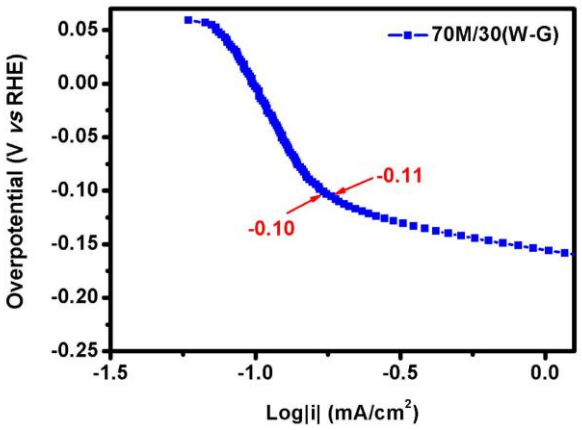

Figure S10. The Tafel plot of 70M/30(W-G) in the region of low current densities.

The onset potential for HER was read from the semi-log (Tafel) plot. For example, the semi-log plot of 70M/30(W-G) in the region of low current densities as displayed in Fig.S8 shows a linear relationship below -0.11V but stars to deviate above -0.10V. Therefore, -0.11 was chosen as the onset potential for 70M/30(W-G). The same method was applied on determining the overpotential for other samples.[5]

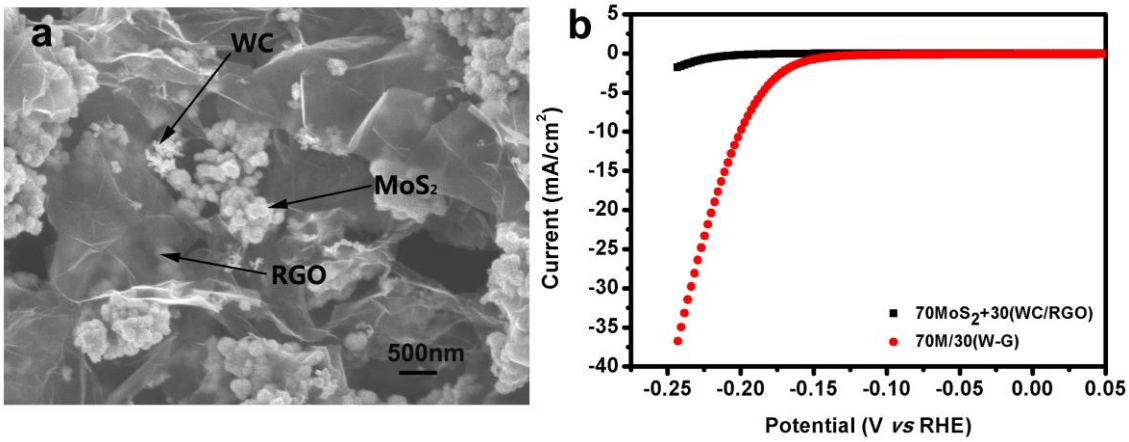

Figure S11. (a) FESEM image of the MoS_2 (70%) particles physically mixed with WC/RGO (30%) and (b) the corresponding polarization curve.

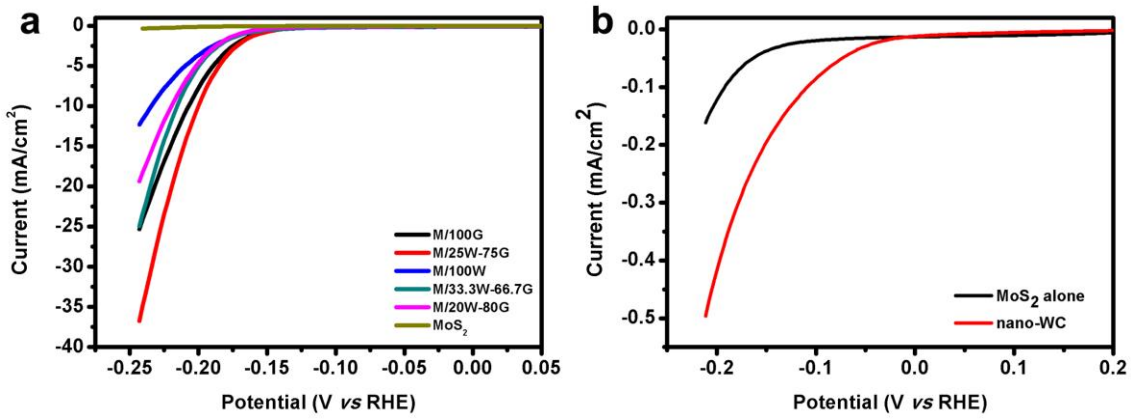

Figure S12. Polarization curve of (a) MoS_2/WC/RGO composites with different WC/RGO ratio in the WC/RGO co-catalyst and (b) nano-WC (MoS_2 was used as a reference).

References

1 Y. Yan, L. Zhang, X. Qi, H. Song, J.-Y. Wang, H. Zhang, X. Wang, *Small* 2012, **8**, 3350.
2 M. C. Weidman, D. V. Esposito, I. J. Hsu, J. G. Chen, *J. Electrochem. Soc.* 2010, **157**, F179.
3 P. N. Ross Jr, P. Stonehart, *J. Catal.* 1977, **48**, 42.
4 Z. Wu, Y. Yang, D. Gu, Q. Li, D. Feng, Z. Chen, B. Tu, P. A. Webley, D. Zhao, *Small* 2009, **5**, 2738.
5 W.-F. Chen, K. Sasaki, C. Ma, A. I. Frenkel, N. Marinkovic, J. T. Muckerman, Y. Zhu, R. R. Adzic, *Angew. Chem. Int. Ed.* 2012, **51**, 6131.